NAVAL POSTGRADUATE SCHOOL
Monterey, California

THESIS

LINK BUDGET ANALYSIS FOR UNDERSEA ACOUSTIC SIGNALING

by

Joseph T. Hansen

June 2002

Thesis Advisor:	Joseph A. Rice
Second Reader:	Kevin B. Smith

Approved for public release; distribution is unlimited

THIS PAGE INTENTIONALLY LEFT BLANK

REPORT DOCUMENTATION PAGE	*Form Approved OMB No. 0704-0188*

1. AGENCY USE ONLY *(Leave blank)*	**2. REPORT DATE** June 2002	**3. REPORT TYPE AND DATES COVERED** Master's Thesis

4. TITLE AND SUBTITLE: Title (Mix case letters) Link Budget Analysis for Undersea Acoustic Signaling	**5. FUNDING NUMBERS**
6. AUTHOR(S) Joseph T. Hansen, LT. USN	
7. PERFORMING ORGANIZATION NAME(S) AND ADDRESS(ES) Naval Postgraduate School Monterey, CA 93943-5000	**8. PERFORMING ORGANIZATION REPORT NUMBER**
9. SPONSORING /MONITORING AGENCY NAME(S) AND ADDRESS(ES) N/A	**10. SPONSORING/MONITORING AGENCY REPORT NUMBER**

11. SUPPLEMENTARY NOTES The views expressed in this thesis are those of the author and do not reflect the official policy or position of the Department of Defense or the U.S. Government.

12a. DISTRIBUTION / AVAILABILITY STATEMENT Approved for public release, distribution is unlimited	**12b. DISTRIBUTION CODE**

13. ABSTRACT *(maximum 200 words)*

Link-budget analysis is commonly applied to satellite and wireless communications for estimating signal-to-noise ratio (SNR) at the receiver. Link-budget analysis considers transmitter power, transmitter antenna gain, channel losses, channel noise, and receiver antenna gain. For underwater signaling, the terms of the sonar equation readily translate to a formulation of the link budget. However, the strong frequency dependence of underwater acoustic propagation requires special consideration, and is represented as an intermediate result called the channel SNR. The channel SNR includes ambient-noise and transmission-loss components. Several acoustic communication and navigation problems are addressed through wideband link-budget analyses.

14. SUBJECT TERMS : Underwater acoustic communication, bandwidth optimization, link budget	**15. NUMBER OF PAGES** 59
	16. PRICE CODE

17. SECURITY CLASSIFICATION OF REPORT	**18. SECURITY CLASSIFICATION OF THIS PAGE**	**19. SECURITY CLASSIFICATION OF ABSTRACT**	**20. LIMITATION OF ABSTRACT**
Unclassified	Unclassified	Unclassified	UL

NSN 7540-01-280-5500 Standard Form 298 (Rev. 2-89)
Prescribed by ANSI Std. 239-18

THIS PAGE INTENTIONALLY LEFT BLANK

Approved for public release; distribution is unlimited

LINK BUDGET ANALYSIS FOR UNDERSEA ACOUSTIC SIGNALING

Joseph T. Hansen
Lieutenant, United States Navy
B.S. Auburn University, 1994

Submitted in partial fulfillment of the
requirements for the degree of

MASTER OF SCIENCE IN ENGINEERING ACOUSTICS

from the

NAVAL POSTGRADUATE SCHOOL
June 2002

Author: Joseph T. Hansen

Approved by: Joseph A. Rice
Thesis Advisor

Kevin B. Smith
Co-Advisor

Kevin B. Smith
Chairman, Engineering Acoustics
Academic Committee

THIS PAGE INTENTIONALLY LEFT BLANK

ABSTRACT

Link-budget analysis is commonly applied to satellite and wireless communications for estimating signal-to-noise ratio (SNR) at the receiver. Link-budget analysis considers transmitter power, transmitter antenna gain, channel losses, channel noise, and receiver antenna gain. For underwater signaling, the terms of the sonar equation readily translate to a formulation of the link budget. However, the strong frequency dependence of underwater acoustic propagation requires special consideration, and is represented as an intermediate result called the channel SNR. The channel SNR includes ambient-noise and transmission-loss components. Several acoustic communication and navigation problems are addressed through wideband link-budget analyses.

THIS PAGE INTENTIONALLY LEFT BLANK

TABLE OF CONTENTS

LIST OF FIGURES

THIS PAGE INTENTIONALLY LEFT BLANK

ACKNOWLEDGMENTS

As my thesis work comes to an end, I wish to thank the following people for their support:

To my lovely wife Tina. In addition to the arduous task of raising our new twins, she has given me the support and motivation to excel.

To my thesis advisor, Joe Rice, who provided me the vision of acoustic networking and spent countless hours working with me to ensure this project was a success.

To my co-advisor, Professor Kevin Smith, who provided support in physics based modeling and thesis preparation.

I extend many thanks to LCDR Peter Duke of the Canadian Navy for his work on the computer code I used as the foundation of my analysis.

I also wish to thank all the staff and students in the Physics and Oceanography curricula for their contributions to my successful completion of this career milestone.

THIS PAGE INTENTIONALLY LEFT BLANK

I. INTRODUCTION

The availability of affordable and sophisticated digital signal processing has enabled modern undersea acoustic communications systems. Advances in this field have opened the door to autonomous sensors and untethered vehicles capable of networked operations in the undersea environment.

There is a great interest in this technology at all levels of the Department of Defense. Autonomous sensors and Unmanned Undersea Vehicles (UUVs) are part of the Defense Department's vision of a joint force capable of rapid data assimilation and unit coordination. In testimony before the Subcommittee on Research and Development of the House Armed Services Committee on Navy Transformation, Vice Admiral Dennis McGinn, Deputy CNO for Requirements and Programs, stated[1],

> Unmanned Undersea Vehicles (UUV) and deployable undersea sensor systems will extend the reach and capabilities of our battlegroup and Marine Air Ground Task Force (MAGTF) commanders by providing essential near-real time data to support ISR requirements independent of, or in concert with, the use of manned platforms or limited Joint Theater or National Assets….Ultimately, with a common integration of networks, sensors, weapons, and platforms, networked warfighters can achieve battlespace dominance through knowledge superiority.

For radio frequency (RF) communications, link budgeting is commonly used to predict system performance in a representative environment. The link budget estimates the signal level at the receiver for a given transmit power and antenna configuration and accounts for environmental factors such as transmission loss and interference.

This paper shows that the link budget can be readily applied to an undersea acoustic communication system using the same principles as the RF link budget. The acoustic link budget combines all terms of the active sonar equation to provide a first order approximation of signal available at the receiver.

[1] McGinn, Dennis, VADM, Deputy CNO (Warfare Requirements and Programs), before the Subcommittee on Research and Development of the House Armed Services Committee on Navy Transformation, Feb. 20, 2002

THIS PAGE INTENTIONALLY LEFT BLANK

II. ACOUSTIC COMMUNICATIONS LINK BUDGET

A. LINK BUDGET

Link budgeting is an established method of analyzing performance in wireless and satellite communications. Link budgets are a design tool to predict signal-to-noise ratio (SNR) at a receiver given system parameters such as transmit power and antenna gain, and channel parameters such as propagation loss and interference. This predicted SNR is compared to a minimum required SNR to obtain a link margin. Equation 2.1 and Figure 1 represent a simplified link budget for wireless communications[2],

$$P_{rcv} = P_{xmt} + G_{xmt} + G_{rcv} + L_s + L_n \ , \qquad (2.1)$$

where

P_{rcv} = Received Power, equivalent to SNR (all quantities in dB),

P_{xmt} = Transmitted Power,

G_{xmt} = Transmitting Antenna Gain,

G_{rcv} =Receiving Antenna Gain,

L_s = Free Space Path Loss, spreading and atmospheric attenuation,

L_n = Noise Factor, environmental noise, and multi-access interference (MAI). MAI is elevation in background noise levels caused by networking activity in the wireless medium.

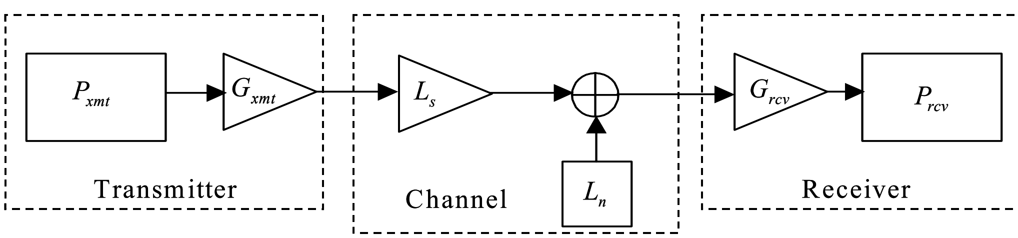

Figure 1. Block diagram representation of the link budget expressed in Equation 2.1.

---

[2] Proakis, John G., (1995). *Digital Communications* (McGraw-Hill, Inc., 1995)

1. Required Signal Level (E_b / N_o)

In digital communications, required signal level is defined as a ratio of energy per bit to receiver noise level, E_b / N_o. This required signal level is a function of the desired nominal bit error rate (BER) for the signaling scheme employed. BER represents the probability of a bit error at the output of the receiver. Figure 2 shows BER as a function of E_b / N_o for a selection of signaling formats.

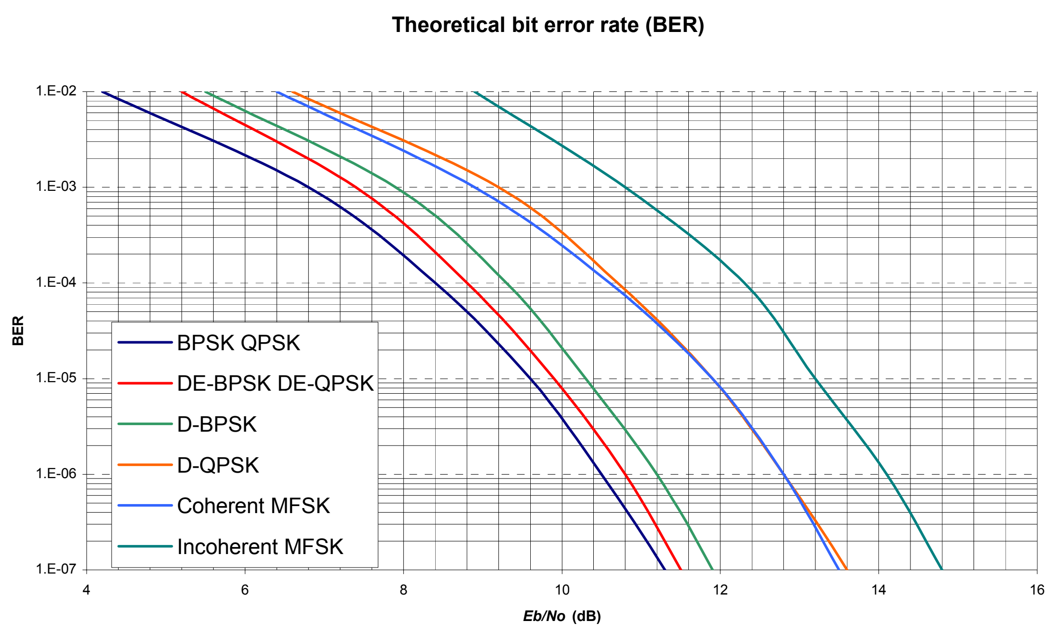

Figure 2. Theoretical bit error rate vs. E_b / N_o for selected modulation schemes. BPSK and QPSK stand for binary and quadrature phase-shift keying respectively. DE refers to differential encoding and D stands for differential demodulation. MFSK is an abbreviation for M-ary frequency shift keying. Data compiled from multiple sources.[3]

[3] Maral, G., Bousquet, M., (1998) *Satellite Communications Systems* (John Wiley and Sons Ltd. 1998), Proakis, John G., (1995). *Digital Communications* (McGraw-Hill, Inc., 1995), and Zyren, Jim, Petrick, Al, (June 1998) *Tutorial on Basic Link Budget Analysis* (Intersil 1998)

2. Available Signal Level

The product of the link budget analysis is available SNR at the receiver. To compare with required E_b / N_o, received power is translated to an energy-per-bit equivalent,[4]

$$\left({E_b}/{N_o} \right)_{rcv} = P_{rcv} * \left({W}/{R} \right) \tag{2.2}$$

where

E_b = Energy required per bit of information,

N_o = Thermal receiver noise in 1 Hz of bandwidth,

R = System data rate,

W = Spectral bandwidth.

Thermal receiver noise level, N_o, is expressed in units of Watts/Hz,

$$N_0 = k_B T_o \tag{2.3}$$

where

$k_B = 1.38 \times 10^{-23}$ W-s/K (Boltzman's constant),

$T_o =$ Receiver temperature in degrees Kelvin.

3. Link Margin

The link margin (LM) compares received E_b / N_o with that required for the established BER,

$$LM = \left(E_b/N_o\right)_{rcv} - \left(E_b/N_o\right)_{req} \quad . \tag{2.4}$$

Although this calculation of link margin has been used primarily in the fields of satellite and wireless communications, this metric is also relevant in predicting performance for an acoustic digital communications system.

---

[4] Zyren, Jim, Petrick, Al, (June 1998) *Tutorial on Basic Link Budget Analysis* (Intersil 1998)

B. ACOUSTIC LINK BUDGET

The process of establishing a link margin for reliable communications is readily applied to the acoustic communications system. The difference is that the terms are now acoustic quantities. Once the acoustic SNR is transformed to an electrical quantity, it can be compared to E_b / N_o to establish a link margin.

1. Directivity Index

The directivity index (DI) may be defined as the ratio of the intensity of a source in some specified direction (usually along the acoustic axis of the source) to the intensity at the same point in space of an omni-directional point source with the same acoustic power. Through the principle of reciprocity, the same principle applies to the receiving transducer. The transmitter and receiver directivity, DI_{xmt} and DI_{rcv}, are analogous to the RF terms for antenna gain.

2. Pressure Spectrum Level

Pressure spectrum level (PSL) is a function of input power and transmission bandwidth. PSL is analogous to SL, but accounts for signal energy distribution over the frequency band of interest. SL is the level expected from a narrow-band tone. For a given input power, SL is estimated by the following equation[5]:

$$SL = 10\log\left(\frac{I_{source@1m}}{I_{ref}}\right) \quad . \tag{2.5}$$

The SL of an omni-directional projector is always referred to a standard range (1 meter) from its acoustic center. At 1 meter the acoustic center of an omni-directional source is surrounded by a sphere of surface area $4\pi r^2 = 12.6m^2$. If the power output is P Watts, then the source intensity at 1 meter is $\frac{P_{xmt}}{12.6} W/m^2$ and SL becomes[6]

$$SL = 10\log\left(\frac{P_{xmt}}{12.6} \times \frac{1}{.67\times10^{-18}}\right). \tag{2.6}$$

[5] Waite, A. D., (1998) *SONAR for Practicing Engineers* (Thompson Marconi Sonar Ltd. 1998)

[6] Waite, A. D., (1998) *SONAR for Practicing Engineers* (Thompson Marconi Sonar Ltd. 1998)

$$SL = 10\log(P_{xmt}) + 170.8 \quad . \tag{2.7}$$

PSL can now be calculated from the given SL. PSL for a pure broadband signal would be represented as

$$PSL = SL - 10 \bullet \log_{10}(W) \tag{2.8}$$

where W is bandwidth in Hz.

For direct sequence spread spectrum (DSSS), the relationship is

$$PSL = SL - 10 \bullet \log_{10}(W) + 10 \bullet \log_{10}(m) \tag{2.9}$$

where m is the number of chippettes. In frequency hopping spread spectrum, one tone is transmitted at a time, therefore PSL=SL. Pressure spectrum level for a multi-frequency shift-keying (MFSK) signal is represented as

$$PSL = SL - 10 \bullet \log_{10}(N) \tag{2.10}$$

where N is the number of tones.

3. Received SNR

The acoustic link budget uses basic sonar theory to estimate the available signal level at the receiver. The basis of the model is the sonar equation,

$$SNR = PSL - TL - AN + DI_{xmt} + DI_{rcv} \tag{2.11}$$

where

SNR = signal to noise ratio at receiver,
PSL = pressure spectrum level of transmitting platform,
TL = transmission loss in the medium,
AN = ambient noise,
DI_{xmt} = transmitter directivity,
DI_{rcv} = receiver directivity.

All quantities are expressed in dB re 1µPa.

Equation 2.12 is analogous to the RF link budget represented in Equation 2.1. Note that the PSL and SNR terms include transmit and receive directivity for simplicity.

Received power in the RF case refers to SNR in acoustic terms, transmitted power corresponds to PSL, directivity index represents antenna gain, and the combination of transmission loss and ambient noise equate to free space path loss and noise terms in the RF link budget equation.

C. CHANNEL COMPONENTS OF THE SONAR EQUATION

1. Transmission Loss

Transmission loss (TL) is a function of source-to-receiver range, r, and is determined by combining the signal loss from source to receiver due to a combination of spreading and attenuation.

Spherical spreading of the signal is assumed to exist up to a range equal to water depth of the channel. Beyond this range, cylindrical spreading is assumed to exist by virtue of the bounded propagation medium. Spherical spreading loss is proportional to $1/r^2$ and is expressed as

$$TL_{sphere} = 20\bullet\log_{10}\left(r\right). \tag{2.12}$$

Cylindrical spreading is proportional to $1/r$ and is expressed as

$$TL_{cylind} = 10\bullet\log_{10}\left(r\right) . \tag{2.13}$$

where r is range in meters.

Attenuation in seawater is caused by three mechanisms: shear viscosity, volume viscosity, and ionic relaxation. As shown by Urick[7], absorption in seawater is frequency dependent and is modeled by the expression

$$\alpha = \frac{0.11 f^2}{1+f^2} + \frac{44 f^2}{4100+f^2} + 3.0\times10^{-4} f^2 + 3.3\times10^{-3} \tag{2.14}$$

where α is the attenuation coefficient in dB/km and f is frequency in kHz.

---

[7] Urick, Robert (1996) *Principles of Underwater Sound for Engineers 3rd. Edition* (Peninsula Publishing, 1996)

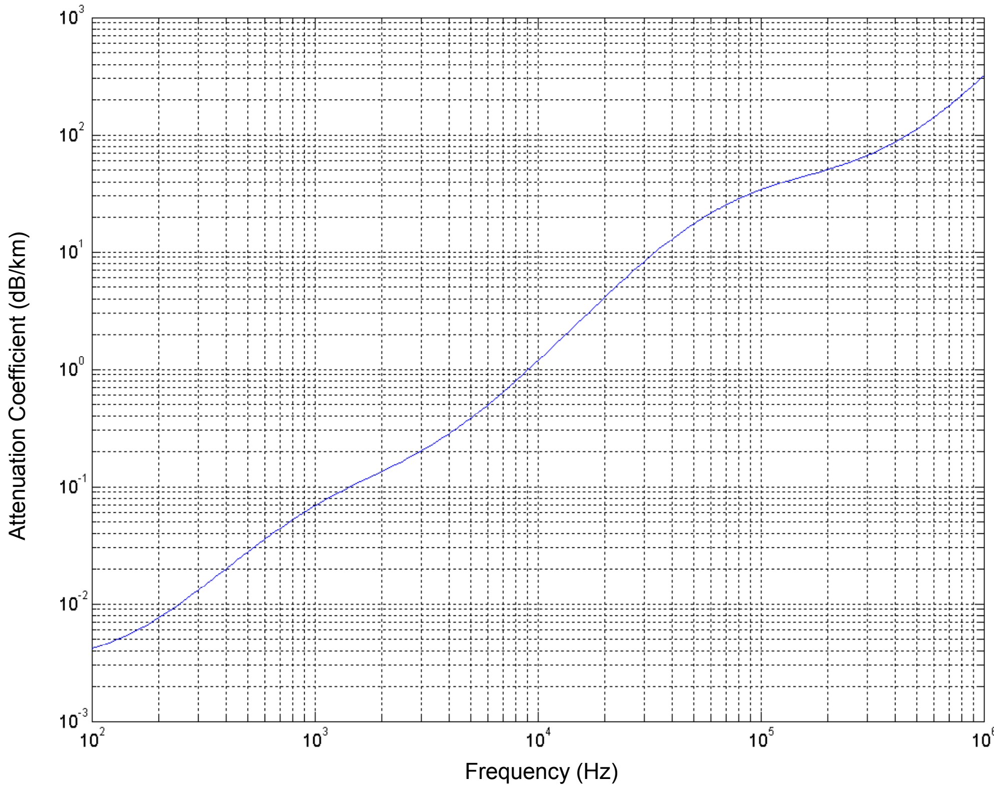

Figure 3. Coefficient for acoustic attenuation in seawater.

The loss due to attenuation in seawater is expressed as

$$TL_{atten} = \alpha r \times 10^{-3} \tag{2.15}$$

where r is range in meters.

Geometric spreading and attenuation are combined to yield total transmission loss (TL). An example of TL is shown in Figure 4. We call attention to the strong dependence on range and frequency. Consider for example, the differential attenuations experienced by 10 kHz and 20 kHz acoustic components where the respective attenuation coefficients are approximately 1 and 4 dB/km, respectively.

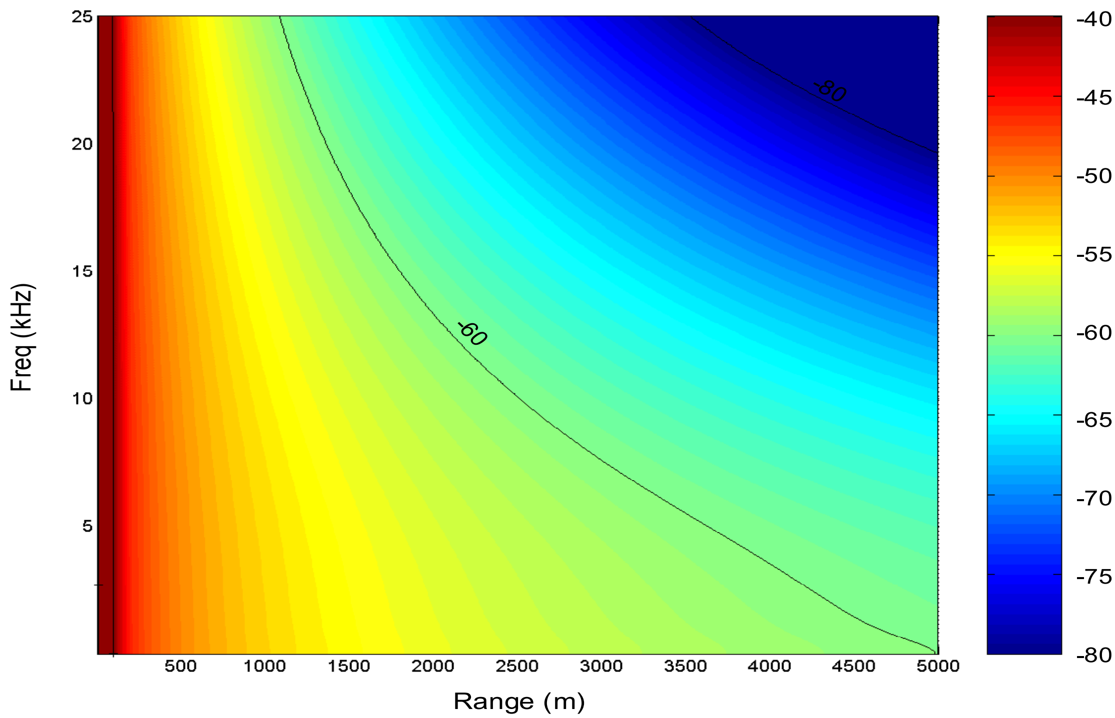

Figure 4. Frequency dependent TL (dB re 1 μPa), plotted as a negative quantity, -TL

2. Ambient Noise

Frequency-dependent ambient noise (AN) can be estimated for various wind speeds and shipping densities using the spectral relationships compiled by Wenz[8]. Figure 5 shows an example noise spectrum for high shipping density and an average wind speed of 10 knots. Again, we observe strong frequency dependence. Because communication frequencies are dominated by wind driven noise, AN varies greatly with wind speed. Figure 6 shows total ambient noise for wind conditions up to 25 kts.

[8] Wenz, G. M., Acoustic Ambient Noise in the Ocean: Spectra and Sources, Journal of the Acoustical Society of America Vol. 34,1936(1962)

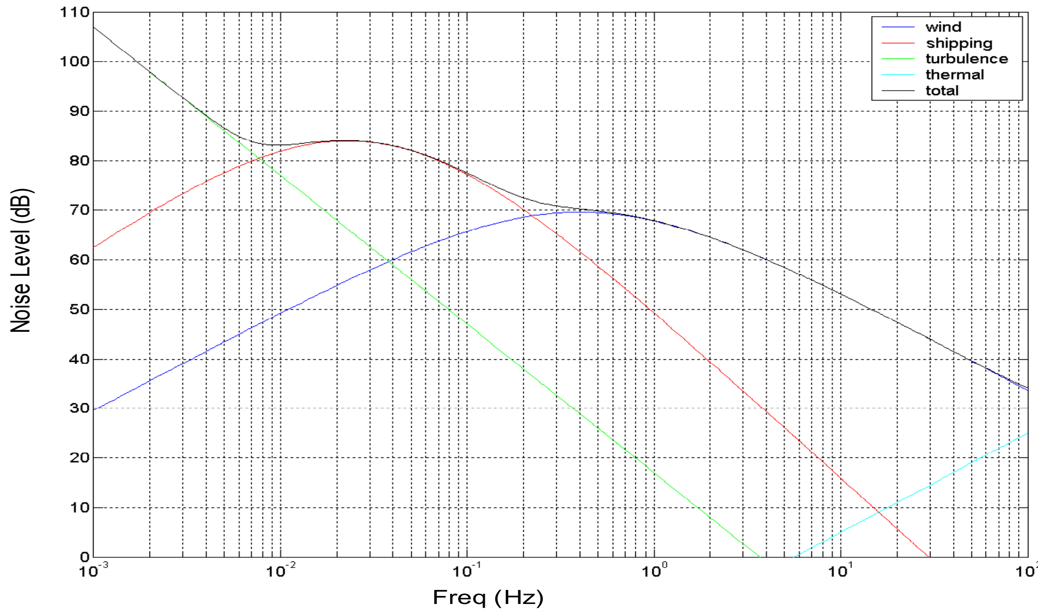

Figure 5. Frequency dependent ambient noise (dB re 1 μPa), with dense shipping and 10 kt winds.

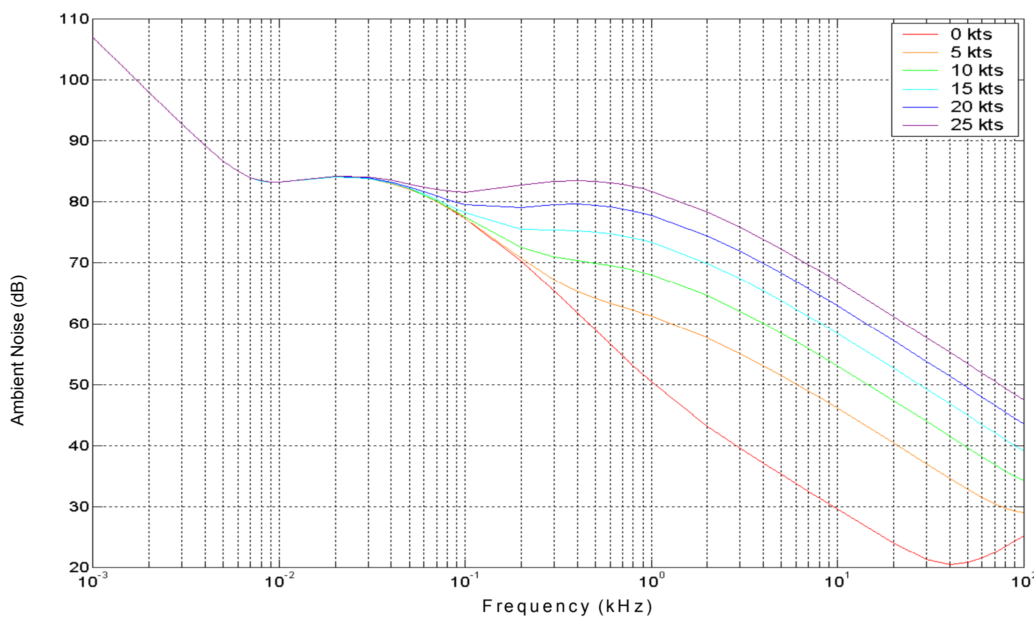

Figure 6. Dependence of total ambient noise on wind speed (dB re 1 μPa).

3. Channel SNR

For acoustic link analysis, an important intermediate result is the gross channel impairment caused by environmental factors. Combining the spreading and attenuation losses with the noise floor, we obtain the link degradation imposed by the propagating medium.

$$SNR_{channel} = -TL - AN \tag{2.16}$$

This channel SNR is naturally normalized to 0 dB and exhibits range and frequency dependence.

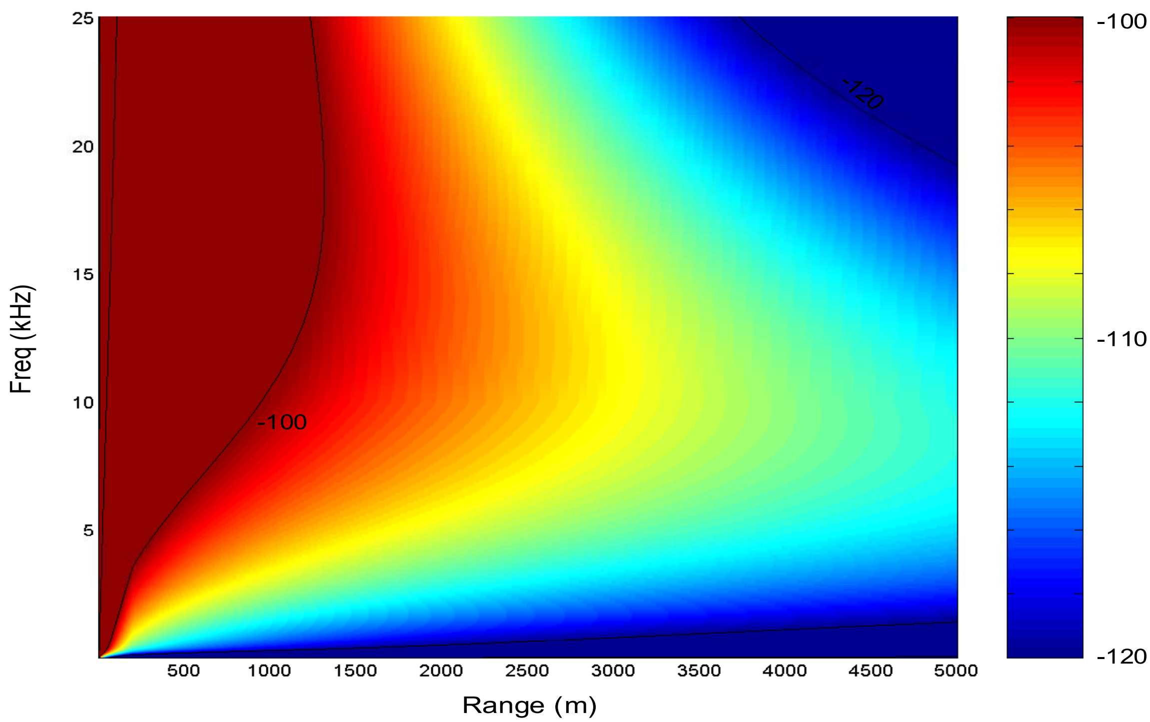

Figure 7. Channel SNR (dB) for a noise environment with heavy shipping and 5 kt. winds.

III. APPLICABILITY OF THE LINK BUDGET

Link budgeting is useful as a design tool where potential environments and system geometries are unknown. However, there are limitations in the accuracy of this approach. With further analysis, the link budget can be adapted to address these issues and improve overall precision.

A. LIMITATIONS

The link budget method of acoustic propagation analysis is a simplified technique providing the analyst with a first-order estimate of link performance. There are inherent inaccuracies that must be considered, all of which require incorporation of physics based propagation modeling.

1. Sound Speed Profile

This model assumes an iso-velocity sound speed profile and therefore ignores the effects of refraction as the sound travels down the channel. Sound speed gradients will cause the signal to undergo more interactions with the surface and bottom as it travels from source to receiver. As discussed in the next chapter, more boundary interactions will lead to further signal reduction that is unaccounted for in the link budget. Shadow zones, another product of sound speed gradients are also unaccounted for.

2. Bottom and Surface Interactions

Losses due to boundary interactions are as of yet not addressed in the acoustic link budget analysis. At the frequencies of interest, surface and bottom interactions are a major loss factor that should be addressed. The Rayleigh criteria evaluates acoustic wavelength relative to the roughness of the sea surface to assess the degree of reflectivity. Frequencies of interest exceed the Rayleigh criteria for all sea states greater than zero. For example, let us assume sea state 1, transmitting frequency of 15 kHz, and a nominal grazing angle of 20 degrees. Wavelength of this signal is 0.1 m and the corresponding wave number is 62.8. Wave height for sea state one is approximately 0.1m We now calculate the Rayleigh parameter[9].

[9] Urick, Robert (1996) *Principles of Underwater Sound for Engineers 3rd. Edition* (Peninsula Publishing, 1996)

$$R = 2kH \sin\theta \,, \tag{3.1}$$

where

R= Rayleigh parameter,

k= wave number,

H= wave height,

θ= grazing angle.

Equation 3.1 represents the ratio of wave height to the z component of wavelength, λ. As wave height becomes large with respect to the z component of signal wavelength, the surface will act more as a scattering interface with increased loss per bounce.

The Rayleigh parameter in this example is 4.2 indicating that the surface should be considered a scattering surface vice a reflective surface. The magnitude of the reflection coefficient is estimated to be

$$\mathbf{R}=\exp(-R). \tag{3.2}$$

The reflection coefficient in this case corresponds to an 18 dB signal loss per bounce at the surface. This example shows that surface attenuation must be considered as a loss term for signals that interact with the sea surface. At shorter ranges and higher frequencies, direct path propagation may be assumed and the Rayleigh criteria may be ignored. When the surface is considered, scattering and bubble interactions will play a large part in signal loss.

Interactions with the sea floor should also be considered for accuracy. The bottom has a number of characteristics similar to the sea surface, but its effects are more complex due to its diverse and stratified composition.[10] The loss per interaction with the bottom is frequency and incident angle dependent due to Rayleigh scattering and the effects of bottom type on the reflection coefficient.

---

[10] Urick, Robert (1996) *Principles of Underwater Sound for Engineers 3rd. Edition* (Peninsula Publishing, 1996)

3. Transducer Directivity

Currently, the link analysis assumes a gross gain afforded by a transducer's directivity index. A more accurate way of representing the directivity term would be to specify a maximum on-axis gain and then express directivity as a function of angle away from the axis of maximum response. The sound velocity profile will have a compounded effect on the directivity, as the sound will be refracted away from the main axis in the presence of a sound speed gradient.

B. COMPARISON WITH PHYSICS-BASED MODEL

To validate the link budget approach to acoustic prediction, we compare it to the results of an established physics-based propagation model. The Monterey-Miami Parabolic Equation (MMPE)[11] uses the parabolic approximation to the wave equation to model acoustic propagation in a wide range of underwater environments.

The MMPE model was used to compute transmission loss in the 0-30 kHz range of frequencies. Channel conditions are selected to closely reflect the assumed channel for link budget analysis. Water depth is 200 m, source and receiver are located at 100 m, sound speed velocity is constant at 1500 m/s, and bottom sound speed is 1700 m/s.

Frequency and range-dependent TL is calculated for the MMPE and link budget. Comparing the two, it is evident that frequency dependent attenuation is unmatched. Both models use identical terms for attenuation coefficient and TL_{atten}. The mismatch is most likely due to the variation in plane-wave path length with frequency. Higher frequencies will attenuate more rapidly along the same path length, but they travel at more shallow grazing angles down the channel than low frequencies. This phenomena results in longer path lengths at lower frequencies for the same range from source to receiver.

The two approaches differ greatly in the variability of transmission loss. The link budget generates a smooth outcome from the application of simple acoustic rules of

[11] Smith, K.B., "Convergence, stability, and variability of shallow water acoustic predictions using a split-step Fourier parabolic equation model," J. Comp. Acoust., Vol. 9, No. 1, pp. 243-285, 2001.

thumb. Conversely, the MMPE model shows as much as 15 dB variance for small changes in range and frequency.

Link budgeting provides a conservative estimate in this case. Further comparison to physics based modeling and real world experiments is warranted to further improve the link budget approach.

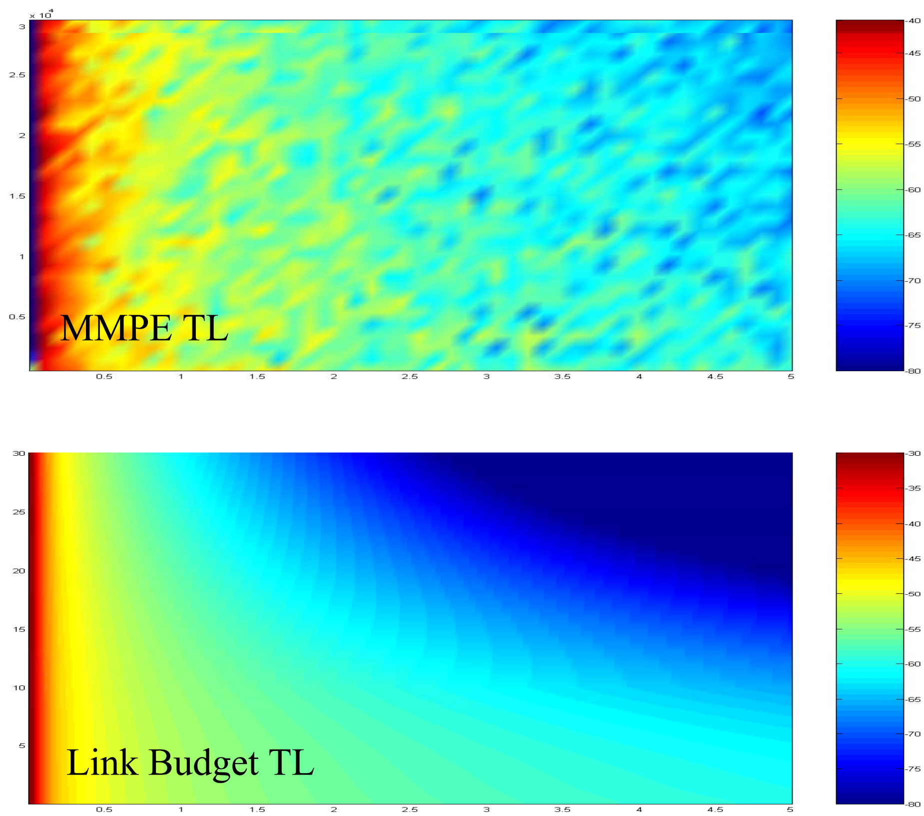

Figure 8. Comparison of TL. MMPE model exhibits less frequency dependency than predicted by link budgeting.

IV. CASE STUDY: TELESONAR DIRECTIVITY

A. INTRODUCTION

In this chapter the utility of the link budget approach to acoustic analysis is shown in a real world design problem. Seaweb is a Navy-sponsored project whose goal is to establish an underwater network capable of reliable digital acoustic communications. Point-to-point links in this network employ telesonar modems. Design criteria require the system to communicate with telesonar link distances up to 5 kilometers. Presently, the system operates at 9-14 kHz using omni-directional transducers. Notice that this band is well matched to the channel SNR plotted in Figure 7.

To enhance network performance, seaweb designers considered using improved transducers with steered directivity. This is accomplished by combining multiple resonant modes of piezo-ceramic cylinders in a controlled manner[12]. In the present telesonar frequency band of 9-14 kHz, the vibrational modes exhibited resonance separations greater than the transmission bandwidth, resulting in poor electroacoustic efficiency.

B. DESIGN TRADE-OFFS

Shifting to the 15-20 kHz frequency band would bring all transducer resonances within the transmission band and provide excellent transmit efficiency. Another advantage of a higher frequency band is reduced transducer size. In addition, multi-user network performance is improved with directional transmitters.

Shifting to a higher frequency band introduces new costs and benefits. A higher frequency will mean increased losses in the medium due to three effects, seawater absorption, surface reflection and scattering losses and bottom reflection and scattering losses. Benefits of shifting to a higher frequency band are a lower ambient noise level and signal gain due to directivity in the transmitting platform. The acoustic link budget is used to estimate the received SNR in both bands for comparison.

---

[12] Butler, A. L., Butler, J. L., Dalton, W. L., Rice, J. A., "Multimode directional telesonar transducer" *Oceans 2000 MTS/IEEE Conference and Exhibition* Vol. 2, pp. 1289-1292

C. LINK BUDGET MODEL AS A COMPARISON TOOL

A link budget analysis is performed for each of the two frequency bands. The directional transducers are expected to provide a directivity index of 9 dB, which is applied uniformly to the 15-20 kHz band. Pressure spectrum level PSL is calculated assuming MFSK modulation and a transmission bandwidth of 5 kHz and is 163 dB for both bands. Figure 9 shows the link budget comparison of received SNR assuming both transducers are omni-directional. Figure 10 shows the improvement we can expect from the directivity term in the 15-20 kHz band.

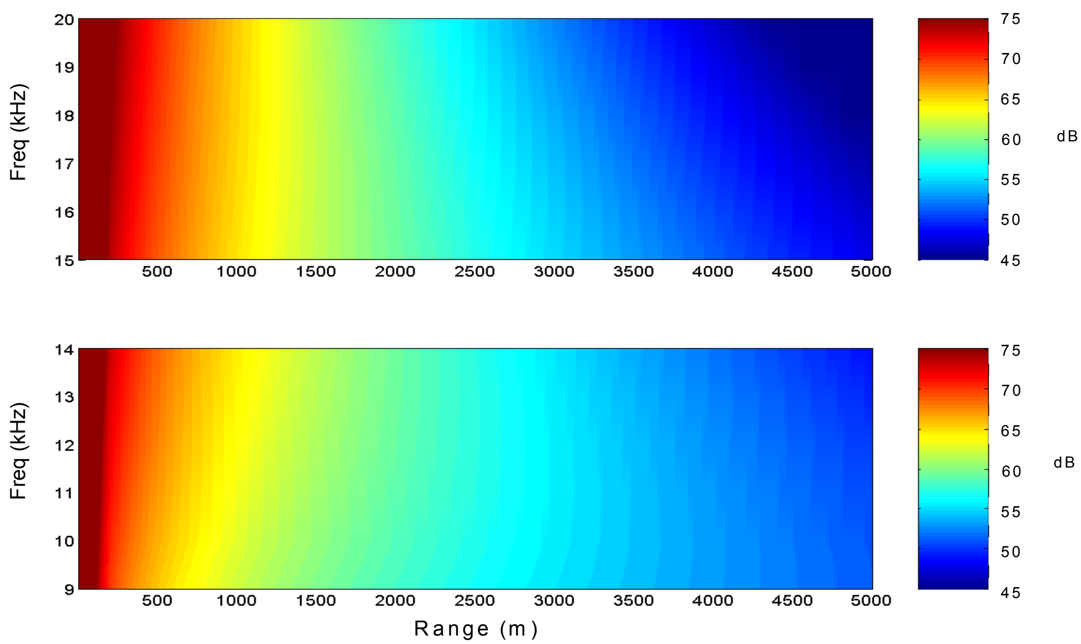

Figure 9. SNR comparison of candidate frequency bands (dB re 1 μPa). Wind speed is 5 kts. Omni-directional transducers are used in both bands.

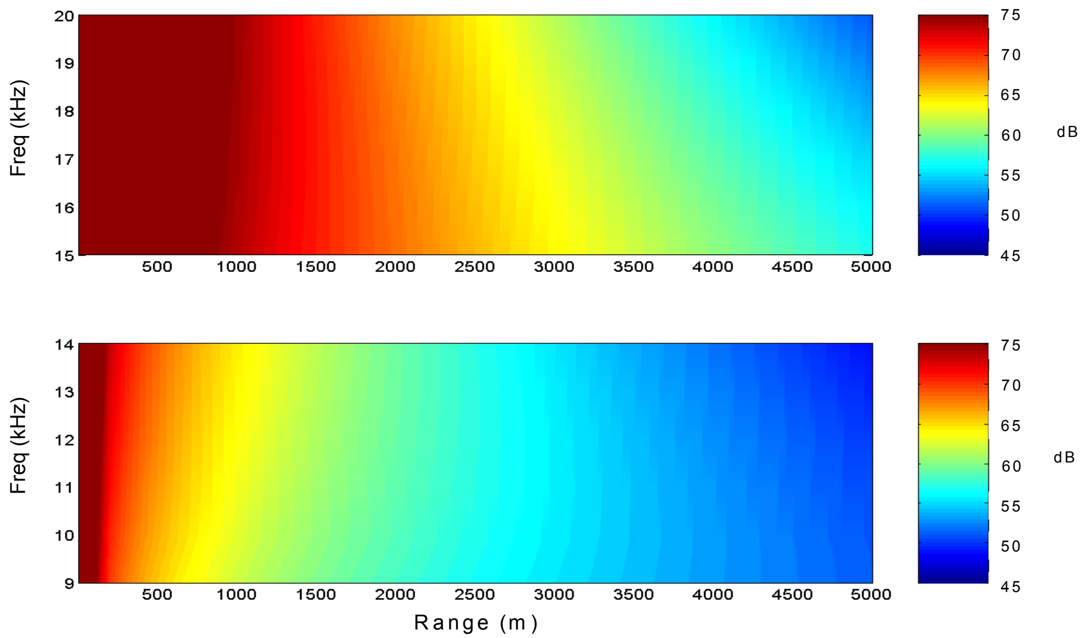

Figure 10. SNR Comparison of candidate frequency bands (dB re 1μPa). Wind speed is 5 kts. 9 dB directivity is employed in the 15-20 kHz band.

D. CONCLUSIONS

Figure 9 shows that increased attenuation at higher frequencies is more detrimental than the decreased noise level is beneficial. Figure 10 shows that adding directivity to the transducer concurrently with shifting to the higher frequency band will result in overall improved SNR at the receiver. From a system perspective, link budget analysis justifies the use of a higher frequency band provided that the implementation of a steered transmitter is practical. Further gains are possible through the use of a directional receiver. A weakness in this analysis is the neglected increase in sound scattering for the higher frequency band as explained in Chapter 3.

THIS PAGE INTENTIONALLY LEFT BLANK

V. CASE STUDY: TELESONAR TRANSMITTER PRE-EMPHASIS

A. INTRODUCTION

Pre-emphasis is the process of spectral weighting at the transmitter to counter the frequency-dependent effects of channel SNR. This case study examines potential benefits of pre-emphasis for spectral equalization of the received SNR. We will select a method of transmitter pre-emphasis based on the channel SNR and observe the resulting link margin.

B. METHOD

For an illustrative example of the process, we consider a communications system designed to operate in the 15-20 kHz frequency band. A design specification of this system will be a bit error rate (BER) of 10^{-6} for noise environments corresponding to a wind speed of 20 kts. Maximum communications range will be 5000 km.

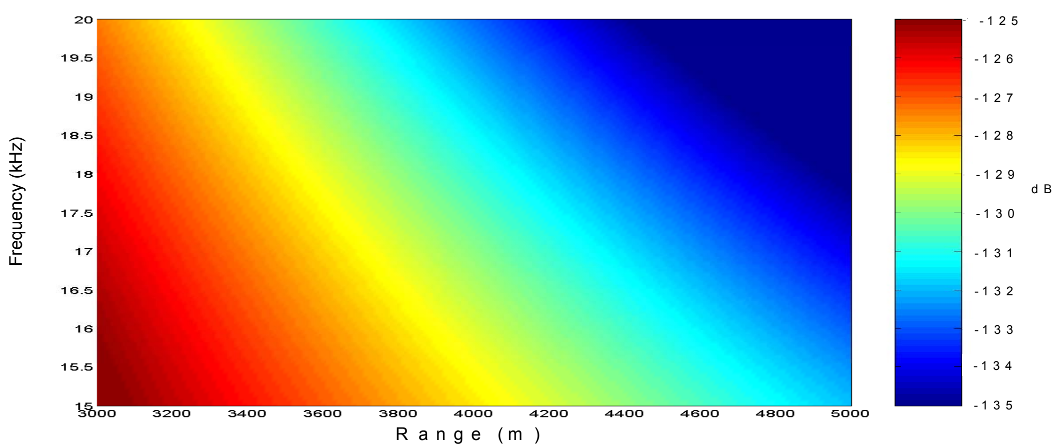

Figure 11. Channel SNR for 20 kts wind speed, exhibiting strong frequency dependence.

We begin by calculating the required receiver SNR for this system. Using a BER of 10^{-6}, we determine the required E_b / N_o for MFSK modulation with incoherent detection using Figure 2. E_b / N_o in this case will be 14 dB. A conservative design would

call for a link margin of 10 dB, therefore the system should be designed so that received E_b / N_o equals 24 dB. This corresponds to an actual ratio of 251:1. Employing Equation 2.2 for R=1200 b/s and W=5000 Hz, we calculate a required power to noise ratio (P_{rcv}) of 60.3:1. Converting to a decibel equivalent yields P_{rcv} =17.8 dB. No directivity is present in the receiver; therefore the required SNR will also be 17.8 dB. We now select a PSL that will achieve the required SNR at mid band.

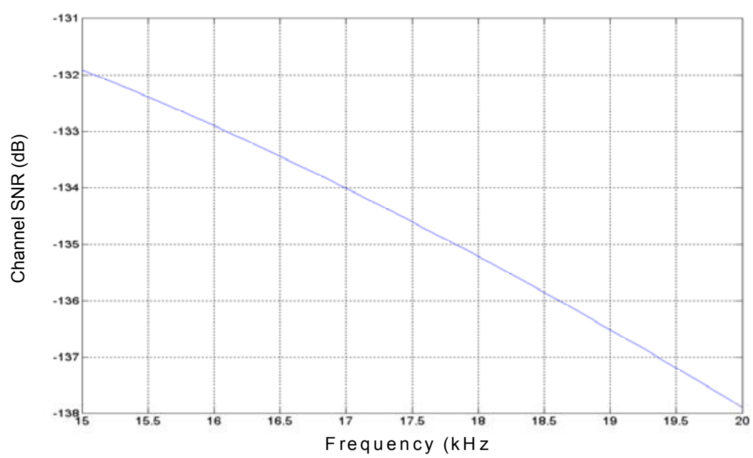

Figure 12. Channel SNR as a function of frequency for r=5000 m and 20 kts wind speed. Channel SNR at mid-band is -134.6. A PSL of 152.4 is required to obtain a received SNR of 17.8 dB.

We apply a PSL of 153 dB uniformly across the spectrum and observe the results. Received SNR is plotted in Figure 13. The uniform PSL results in a region of unsatisfactory reception.

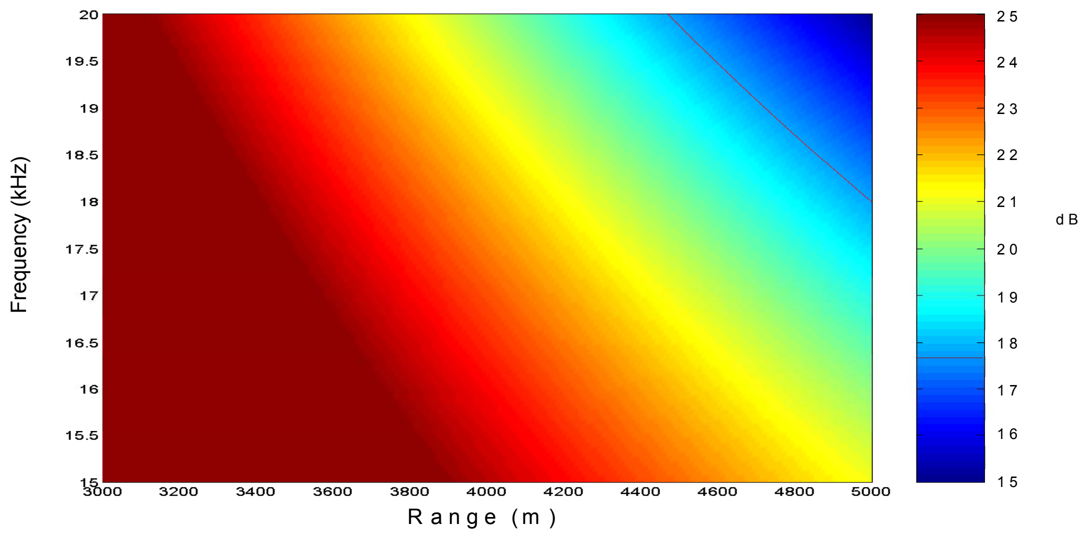

Figure 13. Received SNR for uniform PSL=153 dB. Note that a region of unsatisfactory SNR exists at high frequencies for ranges greater than 4400 m.

Increasing PSL will satisfy system requirements but greater power consumption will result. This is a critical constraint in the design of a network that relies on battery power. Applying pre-emphasis to the transmitter improves response at higher frequencies while maintaining the same average PSL.

Figure 13 suggests that a ramped pre-emphasis will adequately compensate for the transmission losses at higher frequencies. We choose a linear increase of signal strength with frequency as shown in Figure 13.

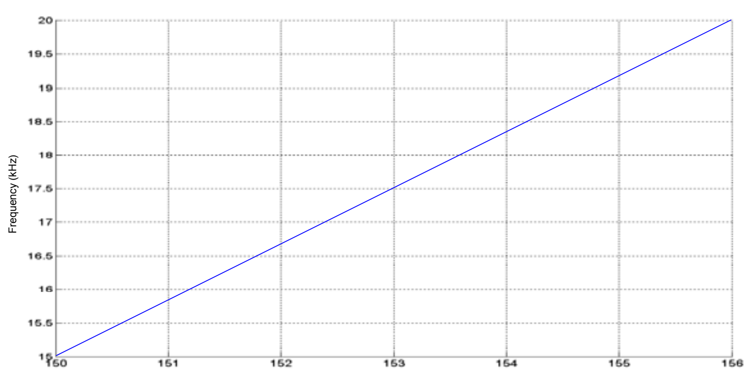

Figure 14. Transmitter pre-emphasis to adjust for greater loss at high frequencies.

C. CONCLUSIONS

Figure 15 compares the received SNR for a flat spectrum transmission to one that employs ramped pre-emphasis. Average PSL is equal in both cases. The system that employs transmitter pre-emphasis exhibits satisfactory SNR throughout the entire region at no additional power cost. The system should operate with the designed BER for wind speeds less than or equal to 20 kts.

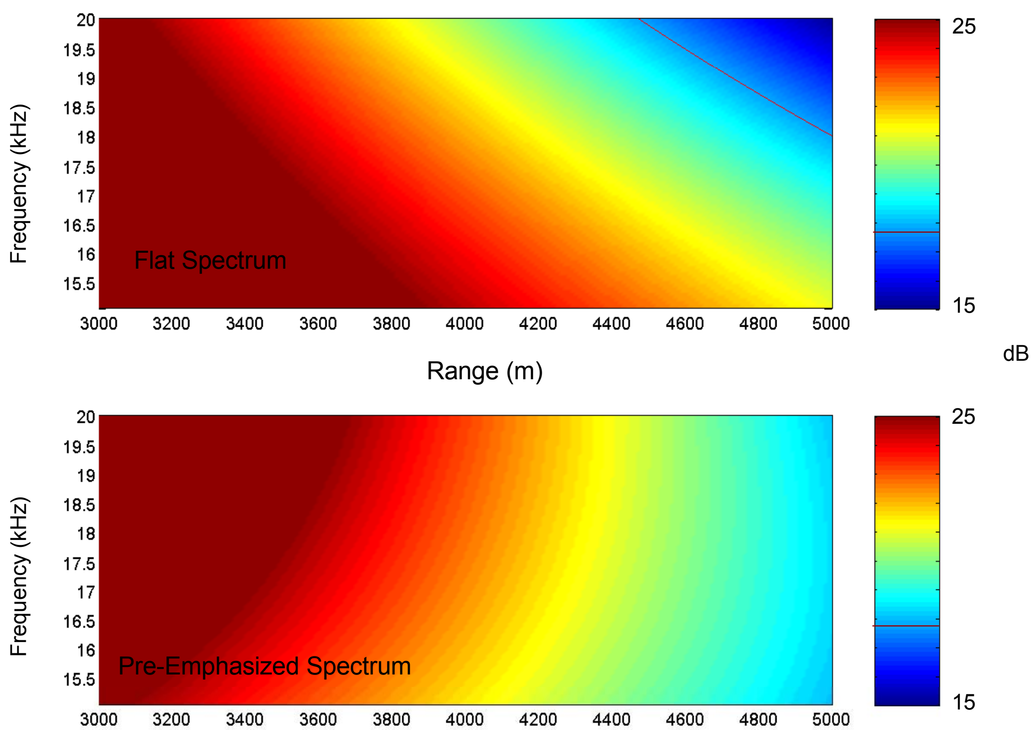

Figure 15. Comparison of received SNR for a flat spectrum source to one with ramped pre-emphasis. Average PSL=153 dB in both cases. Note that the pre-emphasized case shows adequate signal level for all ranges and frequencies at no additional cost in signal power.

VI. CASE STUDY: TELESONAR SHORT-RANGE LINK CAPACITY

Future uses of telesonar modems include underwater acoustic local area networks capable of high bandwidth digital communications. These networks have a wide range of potential uses including surveillance and oceanographic monitoring. Networks would employ shorter link distances and operate at higher frequencies than the present telesonar modems to take advantage of lower noise levels and greater bandwidth. Point-to-point communications in a notional network could range from 10 to 1500 m and employ frequency bands within the 30 to 100 kHz spectrum.

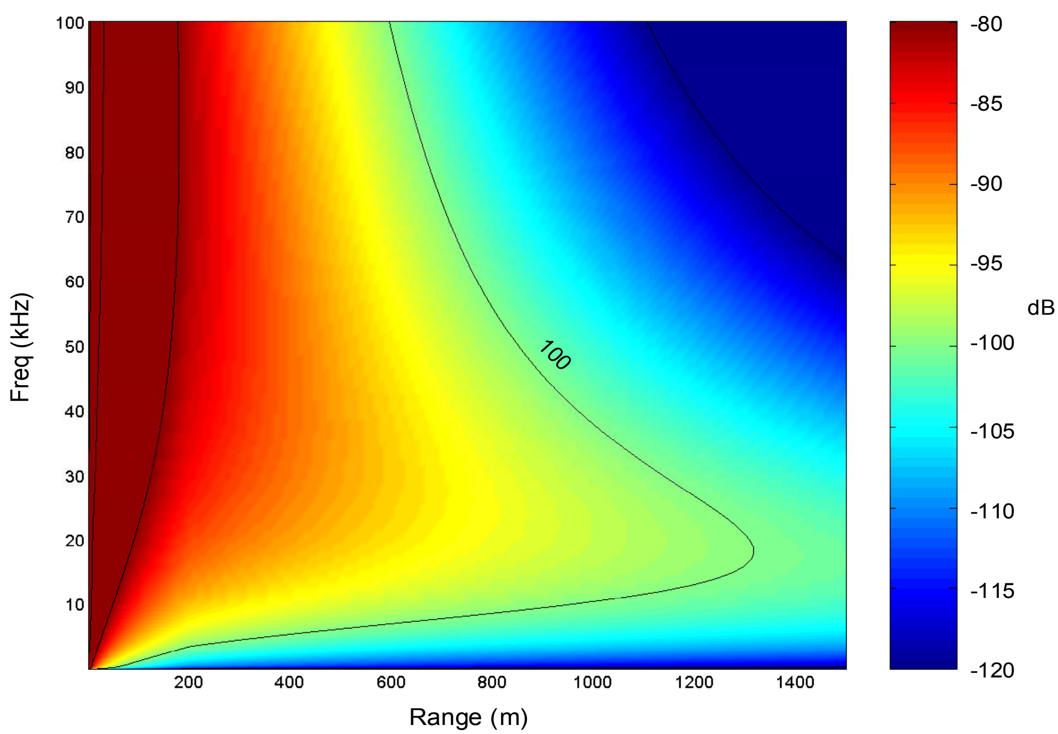

Figure 16. Transmission loss and link performance are highly frequency dependent. As a result, the available transmission bandwidth will vary highly with range for a specific transmit power. This figure shows channel SNR with a wind speed of 5 kts.

A. RANGE DEPENDENT BANDWIDTH

It is desirable to maximize the available communications bandwidth. As Figure 16 shows, bandwidth will be exceedingly range dependent in the frequency bands of interest. Networks could be designed to take advantage of higher available bandwidths for shorter ranges while limiting bandwidth to acceptable limits at longer ranges. Link budget analysis allows us to determine acceptable bandwidth as a function of range. Figure 17 shows a result for 5 kt. wind speed.

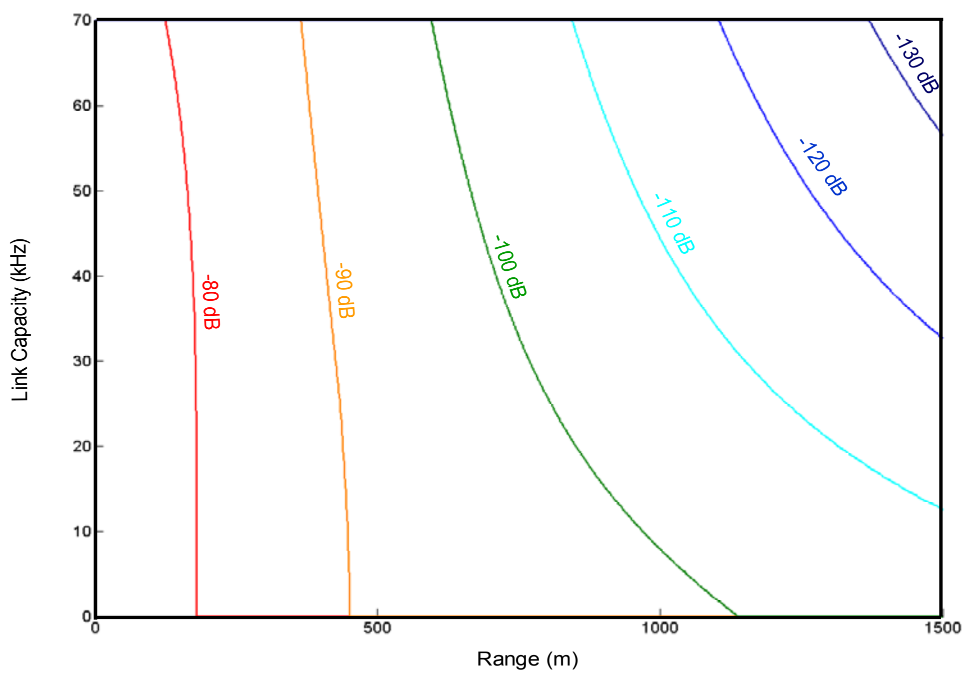

Figure 17. Available bandwidth in the 30-100 kHz spectrum as a function of range for a family of specified channel SNRs. Wind speed is 5 kts.

B. SENSITIVITY TO WIND SPEED

Returning to the link budget expressed in Equation 2.12, one sees that available bandwidth will exhibit a dependence on ambient noise level as well as range. The major contribution to total ambient noise in the frequency bands of interest is wind-driven sea state. Channel SNR and available transmission bandwidth exhibited strong noise dependence as shown below. Wind speed is varied from 0-25 kts and the effects are

shown in Figures 18 and 19. Figure 6 shows wind driven sea state's contribution to total noise.

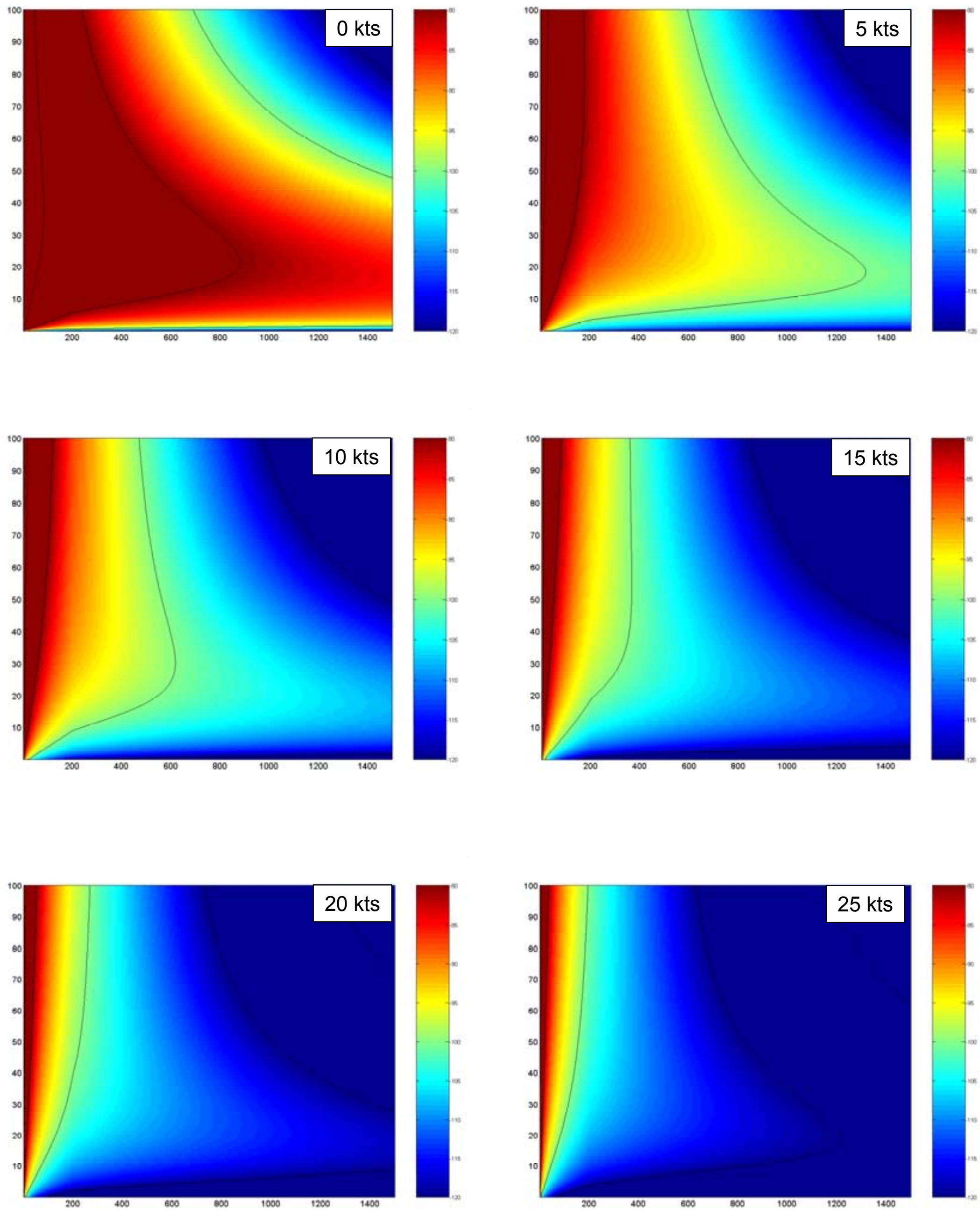

Figure 18. Channel SNR as a function of wind speed.

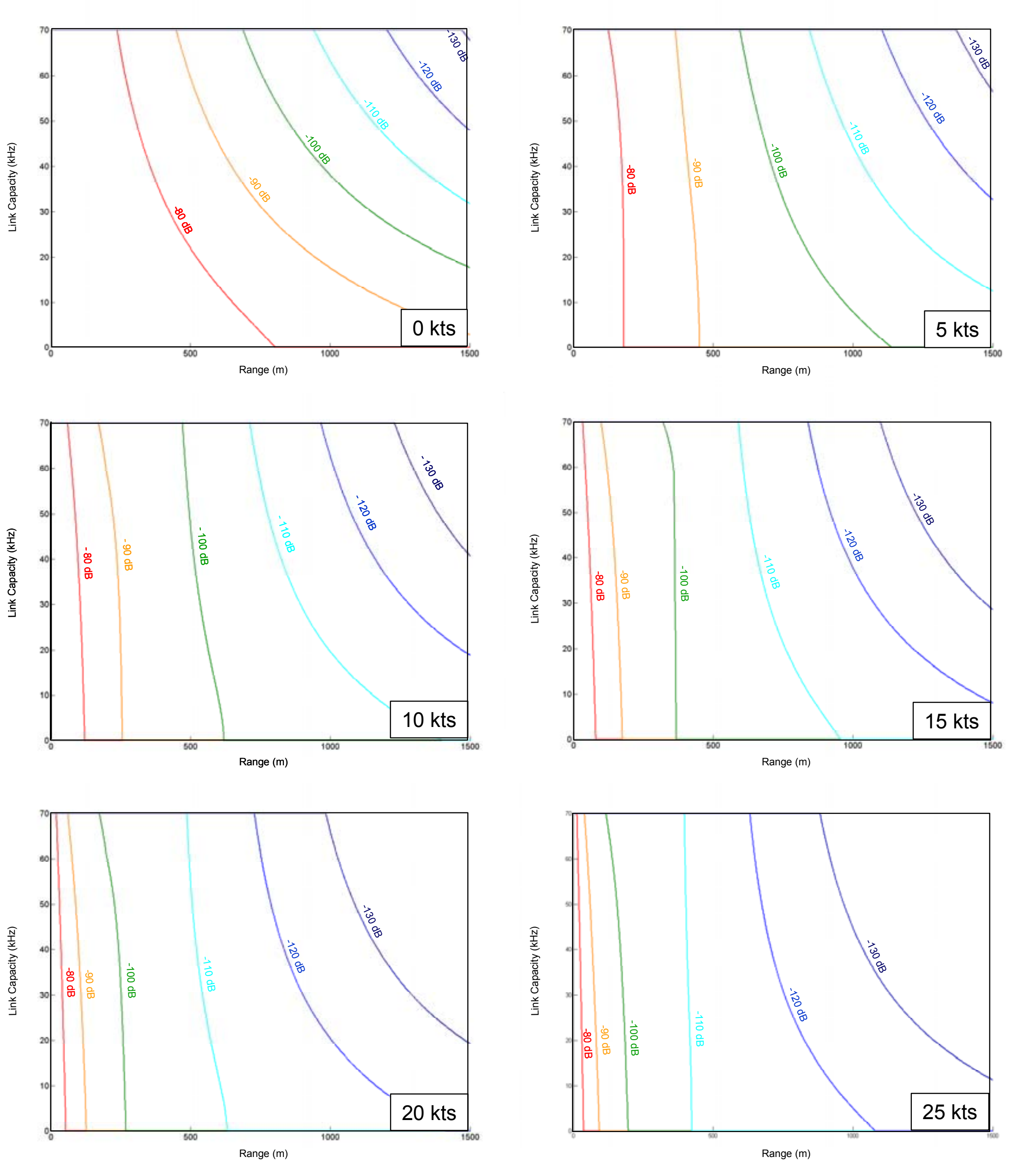

Figure 19. Range-dependent bandwidth in the 30-100 kHz spectrum as a function of wind speed.

C. CONCLUSIONS

Channel conditions in the frequency range of 30-100 kHz are strongly range-dependent due to seawater attenuation and spreading losses. This case study presents a best-case analysis of range dependent propagation loss due to the neglect of surface and bottom scattering and surface bubble effects. Wind speed affects the receiver SNR in two ways. First, higher sea state produces pronounced scattering and bubble effects, increasing transmission loss. Second, wind variations strongly affect the ambient noise level in the frequency band of interest.

THIS PAGE INTENTIONALLY LEFT BLANK

VII. CONCLUSIONS

A. RESULTS

The link budget is applied to an undersea acoustic communication system using the same principles as the RF link budget. The acoustic link budget incorporates terms of the active sonar equation to provide a first-order estimate of signal available at the receiver. Three case studies demonstrated the utility of an acoustic link budget in designing wideband communications systems.

Link budgeting considers the range and frequency dependence of wideband signals in the acoustic medium. In particular, the channel SNR is strongly frequency dependent in the bands of interest.

The link budget is a useful tool in visualizing the channel's influence on the transmitted signal and in assessing the consequences of adapting the transmission strategy.

B. RECOMMENDATIONS FOR FUTURE WORK

A more accurate link budget analysis would not ignore the effects of scattering at the surface and bottom of the communications channel. One possible solution would be an additional term in the attenuation factor based on the mean bottom roughness and sea-state. This term would introduce additional losses due to the scattering effects of boundary interactions. Such a term would also be dependent on the sound speed profile to account for the increase in boundary interactions caused by gradient induced sound refraction.

Physics based modeling could be a potential method of arriving at this additional loss term. Numerous model runs could be performed to develop a statistical average for total transmission loss for variations in sound speed profile, sea-state, and bottom topography.

Real world experiments using wideband signals in shallow water would also be of great use in validating the link budget as an analysis tool.

Link budgeting is useful as a design tool, where the potential environments and system geometries are unknown. As one moves from system design to performance prediction, information about the intended environment and source/receiver geometries should be incorporated into a physics-based numerical propagation model to obtain higher fidelity measurements.

APPENDIX A: MATLAB CODE

MAIN LINK BUDGET PROGRAM

```
%Link Budget Equation
%Thesis Version 3
clear all; clc;
%**********************
%initialize parameters
[f, R, depth, ws, D] = initialize;
%*************************
% Transmission Loss (TL)
disp('calculating TL')
[TL, TLa, TLs, alpha1] = transmissionloss(R, f, depth);
%*****************************
% Noise Level (NL)
disp('calculating NL')
[NLwind, NLship, NLturb, NLtherm, NLtotal, NL] = noiselevel(R,
f, ws, D);
%**********************************
%Source Level
disp('caluclating source level');
[SL] = sourcelevel(R, f);
%**********************************
%Link Margin
disp('calculating the link margin')
linkmargin = SL + TL + NL;
%**********************************
%Calculate the 'Noise' to be overcome
disp('calculating the Noise to be overcome')
relSNR = NL + TL;
%**********************************
%PLOT OUTPUTS
```

```
%*************************
disp('generating plots')
%********************
% %TL plots
allplots('TLplots', R, f, TL, TLa, TLs, alpha1)
% %********************
% %NL plots
 allplots('NLplots', R, f, ws, D, NLwind, NLship, NLturb, NLtherm,
NLtotal, NL)
% %*********************
% %Relative SNR
 allplots('relSNRplots', R, f, ws, D, relSNR)
%********************
%Link Margin plots
allplots('linkmarginplots', R, f, linkmargin)
```

INITIALIZE SUBROUTINE

```
    function [f,R,depth,ws,D,Pe,nu,L] = initialize
%************************
%Initialize Data
%************************
 clear all;
 clc;
%**************************
%Define Range and Frequency Limits:
%frequencies of interest (Hz)
f_upper = 20000;
f_lower = 15000;
f_res = 50;
%ranges and depth (m)
depth = 200;
range = 5000;
```

```
range_res = 10;
%*********************************
%Generate Frequency and Range vectors:
% BW = f_upper - f_lower;
% stop = ceil(log10(f_upper+1));
% for i = 1:stop;
%     f(:,i) = [ (1*10^(i-1)) : (f_res*10^(i-1)): (9.99*10^(i-1)) ]';
% end
% f = reshape(f,9*i/f_res,1);
% begin = find(f==f_lower);
% finish = find(f==f_upper);
%
% f = f(begin:finish);
f=(f_lower:f_res:f_upper);
f=f';
R = [0:range_res:range]; R(1)=1;
%***************************
%Define noise related parameters
%wind speed in m/s
ws=20;
%shipping activity low (D=0), med (D=0.5), high (D=1)
D=1;
```

TRANSMISSION LOSS SUBROUTINE

```
function [TL, TLattenuation, TLspreading, alpha1] = transmissionloss(R, f, depth)
%*************************
% TRANSMISSION LOSS
%****************************************
%TL due to Spreading - Matrix (Range x Freq)
Rindex1 = find(R==depth);   %max range of spherical spreading
```

```
%Rindex2 = find(R==depth);     %max range of transitional spreading
Rindex3 = find(R==depth);  %max range of cylindrical spreading
TLspreading1 = 20*log10(R(1:Rindex1));
TLspreading3 = (10*log10(R(Rindex1+1:end))-10 *log10(R(Rindex1))) + TLspreading1(end);
TLspreadingtotal = [TLspreading1 TLspreading3];
TLspreading = TLspreadingtotal;
for findex = 2:length(f)
   TLspreading = [TLspreading; TLspreadingtotal];
end
%*******************************************
%TL due to Attenuation - Matrix (Freq x Range)
%using eqn from Urick p 108
%note this is given in dB/kyd with f in kHz therefore need to convert
fkhz = f./1000;
alpha1 = ((0.11.*(fkhz.^2)) ./ (1 + (fkhz.^2))) + ((44.*(fkhz.^2)) ./ (4100 + (fkhz.^2))) + ((3.0.*(10.^(-4))).*(fkhz.^2)) + 0.0033;
for Rindex = 1:length(R)
   for findex = 1:length(f);
      TLattenuation(findex,Rindex) = alpha1(findex).*R(Rindex).*1e-3;
   end
end
%********************************************
%Total Transmission Loss Matrix
TL = TLattenuation + TLspreading;
TL=-TL;
```

NOISE LEVEL SUBROUTINE

```
function [NLwind, NLship, NLturb, NLtherm, NLtotal, NL] = noiselevel(R, f, ws, D)
	%*****************************
	% NOISE LEVEL
	%******************************
	fkhz = f./1000;
	%*******************
	%NL due to Surface Waves Option 2 frin
	NLwind = ( 50 + (7.5.*(ws.^0.5)) + (20.*log10(fkhz)) - (40.*log10(fkhz + 0.4)) );
	%NL due to Shipping
	NLship = ( 40 + (20.*(D-0.5)) + (26.*log10(fkhz)) - (60.*log10(fkhz + 0.03)) );
	%NL due to Turbulence
	NLturb = ( 17 - (30.*log10(fkhz)) );
	%NL due to thermal noise in the receiver
	NLtherm = ( -15 + (20.*log10(fkhz)) );
	%Rain
	%Industrial Noise
	%Biologics
	%**********************
	%Total Noise Level
	NLtotal = 10.*log10( (10.^(NLwind./10)) + (10.^(NLship./10)) + (10.^(NLturb./10)) + (10.^(NLtherm./10)) );
	NL = NLtotal;
	for Rindex = 2:length(R)
	   NL = [NL NLtotal];
	end
	NL=-NL;
```

SOURCE LEVEL SUBROUTINE

```
function [SL] = sourcelevel(R, f)
%*****************************
% Source Level
%******************************
%SL = 171.5 + 10.*log10(Pe) + 10.*log10(nu);
SL=153
SL = SL.*ones(length(f),length(R));
```

PLOTS SUBROUTINE

```
function varargout = allplots(plots,varargin)
switch plots
case 'TLplots'
   R=varargin{1};   f=varargin{2};   TL=varargin{3};
TLa=varargin{4}; TLs=varargin{5}; alpha1=varargin{6};
   figure(1)
   semilogx(R,TLs(1,:)); title('TLspreading'); grid on;
   xlabel('Range (m)'); ylabel('dB');
   figure(2)
   semilogy(f/1000,alpha1);
   %title('attenuation coeff');
   grid on;
   xlabel('Freq (kHz)'); ylabel('dB/Km');
   xlim([1 100]);
   figure(3)
   pcolor(R,f/1000,TLa);
   shading interp;
   colorbar;
   hold on;
   [cs, h] = contour(R, f/1000, TLa, [-100:10:200], 'k');
   clabel(cs);
```

```
        xlabel('Range (m)'); ylabel('Freq (kHz)'); zlabel('dB');
        %title('TLattenuation in dB');
        grid on;
        hold off;
        grid on;
        figure(4)
        pcolor(R,f/1000,TL);
        caxis([-80 -40])
        shading interp;
        colorbar;
        hold on;
        [cs, h] = contour(R, f/1000, TL, [-200:20:200], 'k');
        %clabel(cs);
        %xlabel('Range (m)'); ylabel('Freq (kHz)'); zlabel('dB');
        %title('TL total in dB');
        hold off;
        grid on;
    case 'NLplots'
        R=varargin{1}; f=varargin{2}; ws=varargin{3}; D=varargin{4};
NLwind=varargin{5}; NLship=varargin{6};
        NLturb=varargin{7};                    NLtherm=varargin{8};
NLtotal=varargin{9}; NL=varargin{10};
        figure(5)
semilogx(f/1000,NLwind,'b',f/1000,NLship,'r',f/1000,NLturb,'g',f/1000,NL
therm,'c',f/1000,NLtotal,'k');
        %title('NL');
        grid on;
        %xlabel('Freq (kHz)'); ylabel('dB');
        legend('wind', 'shipping', 'turbulence', 'thermal', 'total');
        ylim([0 110]);
        xlim([0 100]);
        %gtext({sprintf('wind speed: %2.1f m/s', ws),...
            %sprintf('Shipping coeff (D): %2.1f', D)});
```

```
    %   figure(6)
    %   semilogx(f/1000,NLtotal); title('NLtotal in dB'); grid on;
    %   xlabel('Freq (kHz)'); ylabel('dB');
    %

    case 'relSNRplots'
      R=varargin{1}; f=varargin{2}; ws=varargin{3}; D=varargin{4};
relSNR=varargin{5};
    %   figure(7);
    %       R1k=R(11);  R2k=R(21);  %R5k=R(51);  R10k=R(101);
R20k=R(201);
    %   plot(f/1000,relSNR(:,11),'k',f/1000,relSNR(:,21),'g');
    %   %,f,relSNR(:,51),'b',f,relSNR(:,101),'c',f,relSNR(:,201),'r');
    %   grid on;
    %   xlabel('Freq (kHz)'); ylabel('dB');
    %   %title('Total Envirnmentals to Overcome');
    %   legend('1 km', '2 km', '5 km', '10 km', '20 km');
    %   %gtext({sprintf('wind speed: %2.1f m/s', ws),...
    %    %     sprintf('Shipping coeff (D): %2.1f', D)});
      figure(8)
      pcolor(R,f/1000,relSNR);
      shading interp;
      caxis([-160 -120]);
      colorbar;
      hold on;
      %[cs, h] = contour(R, f/1000, relSNR,[-200:20:200],'k');
      %clabel(cs);
      %xlabel('Range (m)'); ylabel('Freq (kHz)'); zlabel('dB');
      %title('Total Environmentals to Overcome in dB');
      hold off;
    case 'linkmarginplots'
      R=varargin{1}; f=varargin{2}; linkmargin=varargin{3};
```

```
    figure(9)
    pcolor(R,f/1000,linkmargin);
    shading interp;
    colorbar;
    hold on;
    [cs, h] = contour(R,f/1000, linkmargin, [17.8 17.8], 'r');
    %clabel(cs);
    xlabel('Range (m)'); ylabel('Freq (kHz)'); zlabel('dB');
    %title('Link Margin in dB');
    hold off;
end
```

PRE-EMPHASIS EXAMPLE SUBROUTINE

```
    %Equalizer: Determines ramped window from bottom to top of band
to apply as source level to the link budget
    fl=15000;              %limits of frequency band
    fu=20000;
    m=find(f>fl);
    n=find(f==fu);
    fr2=f(m:n);            % band vector
    relSNR2=relSNR(m(1):n,:);  % channel SNR for the band of interest
    low=150;               % low end of pre-emphasis
    high=156;              % high "
    % The following creates the weighted source level matrix
    EQ=linspace(low,high);
    XX=ones(max(size(EQ)),length(R));
    for i=1:100;
        EQ2(i,:)=XX(i,:).*EQ(i);
    end
    link2=relSNR2+EQ2;
    linkmargin2=linkmargin(m:n,:);
    % Output plot
```

```
figure;
subplot(2,1,1)
pcolor(R,fr2/1000,linkmargin2);
caxis ([15 25]);
shading interp;
xlim([3000 5000]);
colorbar;
hold on;
[cs,h]=contour(R,fr2/1000, linkmargin2,[17.8 17.8], 'r');
subplot(2,1,2);
pcolor(R,fr2/1000,link2);
shading interp;
caxis([15 25]);
xlim([3000 5000]);
colorbar;
hold on;
[cs h]=contour(R,fr2/1000,link2,[17.8 17.8],'r');
```

LIST OF REFERENCES

Albers, V. M., (1963) *Underwater Acoustics* (Plenum Press, New York 1963)

Ali, H. B., (1993) "Oceanographic Variability in shallow-water acoustics and the dual role of the sea bottom" *IEEE J. Oceanic Eng., Vol. 18, no. 1, pp. 31-41, January 1993*

Brown, W. E., Newcomb, D. R., Bartlett, M. L., Rayborn, G. H., *Estimation of Ocean Bottom Scattering Strength Using Discrete Eigenray Matching in Shallow Water*

Burdic, William S., (1984) *Underwater Acoustic System Analysis* (Prentice-Hall Inc., 1984)

Butler, A. L., Butler, J. L., Dalton, W. L., Rice, J. A., "Multimode directional telesonar transducer" *Oceans 2000 MTS/IEEE Conference and Exhibition* Vol. 2, pp. 1289-1292

Dahl, Peter H., (2001) "High Frequency Forward Scattering from the Sea Surface", *IEEE Journal of Oceanic Engineering*, Volume 26, Number 1, pp. 141-151

Fruehauf, N., Rice, J. A., "System Design aspects of a steerable directional acoustic communications transducer for autonomous undersea systems" *Oceans 2000 MTS/IEEE Conference and Exhibition*, Vol. 1, pp. 565-573

Jensen, F. B., Kuperman, W. A., Porter, M. B., Schmidt, H., (2000) *Computational Ocean Acoustics* (Springer-Verlag New York Inc. 2000)

Jensen, F. B., Kuperman, W. A., "Optimum frequency of propagation in shallow water environments" *Journal of the Acoustical Society of America* Vol. 73, Issue 3, pp. 813-819

Kinsler, L. E., Frey, A. R., Coppens, A. B., Sanders, J. V. (2000). *Fundamentals of Acoustics* (John Wiley & Son, Inc., 2000).

Medwin, Herman, Clay, Clarence S., (1998). *Fundamentals of Acoustic Oceanography* (Academic Press 1998)

Pace, N. G., *High Frequency Acoustics in Shallow Water, call for papers* Conference organized by NATO SACLANT Undersea Research Center, June 1997

Proakis, John G., (1995). *Digital Communications* (McGraw-Hill, Inc., 1995)

Proakis, J. G., Sozer, E. M., Rice, J. A., Stojanovic, M., “Shallow water acoustic networks” *IEEE Communications Magazine* Nov. 2001, Vol. 38, Issue 11, pp. 114-119

Rappaport, T. S., (1996) *Wireless Communications* (Prentice-Hall Inc. 1996)

Rice, Joseph A., *Seaweb Network for FRONT Oceanographic Sensors*, FY01 Report submitted to ONR 321BC, Oct. 2001

Smith, K.B., “Convergence, stability, and variability of shallow water acoustic predictions using a split-step Fourier parabolic equation model,” J. Comp. Acoust., Vol. 9, No. 1, pp. 243-285, 2001.

Sozer, Ethem M., Stojanovic, Milicia, Proakis, John G., “Undersea Acoustic Networks”, *IEEE Journal of Oceanic Engineering Vol. 25 No. 1, January 2000*

Urick, Robert (1986) *Ambient Noise in the Sea* (Peninsula Publishing Los Altos, California 1986)

Urick, Robert (1996) *Principles of Underwater Sound for Engineers 3rd. Edition* (Peninsula Publishing, 1996)

Urick, Robert (1979) *Sound Propagation in the Sea* (Defense Advanced Research Projects Agency 1979)

Waite, A. D., (1998) *SONAR for Practicing Engineers* (Thompson Marconi Sonar Ltd. 1998)

INITIAL DISTRIBUTION LIST

1. Defense Technical Information Center
   Ft. Belvoir, Virginia

2. Dudley Knox Library
   Naval Postgraduate School
   Monterey, California

3. Joseph A. Rice, Code PH/Sk
   Department of Physics
   Naval Post Graduate School
   Monterey, CA

4. Prof. Kevin B. Smith, Code PH/Sk
   Department of Physics
   Naval Post Graduate School
   Monterey, CA

5. LT Joseph T. Hansen
   347 Ardennes Circle
   Seaside, CA 93955